The University of Tehran Press

Pollution

https://jpoll.ut.ac.ir/

Print ISSN: 2383-451X
Online ISSN: 2383-4501

Modeling Convective Cloud Movement Countering with Mountain Peak due to Thermal Pollution and Evaluate Affecting Indexes, A Review on Factors Affecting Climate Change

Siamak Boudaghpour✉

Environment Engineering, Civil Engineering Department, K.N Toosi University of Technology Tehran, Iran

Article Info

Article type:
Research Article

Article history:
Received: 5 October 2024
Revised: 28 November 2024
Accepted: 16 January 2025

Keywords:
Cloud
Numerical modeling
Thermal effects
Convective movement

ABSTRACT

Thermal pollution which causes air movement, has received special attention under different climate conditions. Evaluating the conventional movement in dormant air behind the mountain due to temperature diversion and considering reign wind, two dimensions with turbulent RNG k-ε model were used through Fluent software. Movement in unstable weather conditions and cloud presence were evaluated at a height of 100 to 300 m from the valley base on a spring day. In this model, translocation evaluation is concentrated due to a temperature difference caused by thermal pollution in the mountain slope and valley floor with the adjacent air (conventional flow); in this way, clouds move with air convection. Certainly, the measurement and evaluation of atmospheric statues under the desired conditions had special sensitivity. The aim of this study was to model the effect of meteorological indices on convective movement, such as temperature and speed, under different atmospheric conditions; then, a better understanding was obtained by determining how these movements form weather changes in a specific area. In conclusion, it was shown that temperature differences caused by thermal pollution in the cloud sub-layer in divers' height and cloud localization in the proper profile of wind speed, caused cloud translocation and containing wind in cloud elevation area occurred rapidly in higher levels.

Cite this article: Boudaghpour, S. (2025). Modeling Convective Cloud Movement Countering with Mountain Peak due to Thermal Pollution and Evaluate Affecting Indexes, A Review on Factors Affecting Climate Change . *Pollution*, 11(2), 550-559.
https://doi.org/10.22059/poll.2024.383573.2600

DOI: https://doi.org/10.22059/poll.2024.383573.2600

INTRODUCTION

The Nature of Convection due to buoyancy force formation due to temperature change was studied from a theoretical and experimental point of view in more detail. In recent years, these phenomena have been evaluated using high-speed computers with overhead capacities. mountains cover 1/5th of the earth. Many parts of Iran have also been introduced. As we know, in mountain area clouds, humid weather heightens due to lower density, is cooled, and is concentrated mostly from west to east in the Iran climate. As a result of this process, most clouds do not have the ability to make perceptions and leave more than 90% of their humidity in air. In most cases, clouds are driven around after reaching upper levels or by wind, or remain emotionless or prohibited by obstacles that the mountains are the most important ones. Therefore, air movement and clouds in this area require further investigation. The aim of this study was to numerically model air convection movement and cloud translocation due to temperature differences in their sub-layers, where the possibility of passing these clouds through barriers has been studied. In this assay, the northern part of the country, which is the location with the highest summit, was evaluated.

*Corresponding Author Email: *bodaghpour@kntu.ac.ir*

MATERIAL & METHODS

The main weakness of statistical models in the Atmospheric Sciences assay is their inability to calculate the wind speed profile and constantly estimate the turbulent diffusion coefficient. In the modeling procedure applied in this study, the fluid motion space was divided into smaller components (mesh), and partial derivative equations-defined flow (which is properly demonstrated by Navier–Stokes equations) was applied for all meshes (controlled volume). Therefore, several nonlinear models were obtained, which should be solved simultaneously. For such problems, the flow created is turbulent. In addition to the above equations, other equations would be necessary to pattern the turbulent flow. The results of the modeling include comprehensive flow properties, such as speed, pressure, and compartment concentration, in all solved domains. The study area was one of the Alborz Mountains in the north of the country, where the intended mountain had a height of 1000 m from the valley baseline to the summit. The experimental conditions were associated with one spring day with unstable climate conditions, where the temperature declined logarithmic-ally from 282 K base state. The environmental pressure was equal to 759.3 m bar in station alignment, and the mass ratio of water vapor (cloud) to air was 0.063. Solar radiation was 7.6, cloud coverage was 5N and wind speed was calculated as insignificant in this region.

As in this study, the mass transition evaluated in air and air density was considered fixed owing to the slight change and lower calculation. Therefore, with the assumption that air is a Newtonian Fluid with constant density and theory, the equations of mass survival equality, momentum, and energy were solved in this environment. The transition process in the atmosphere, which encompasses two directional changes, is often modeled through the distribution and transmission equation derived by this formula. Both procedures were separate from the general trend of atmospheric changes.

$$\rho\left(\frac{\partial V_x}{\partial t}+V_x\frac{\partial V_x}{\partial x}+V_y\frac{\partial V_x}{\partial y}\right)=-\frac{\partial p}{\partial x}+\mu\left(\frac{\partial^2 V_x}{\partial x^2}+\frac{\partial^2 V_x}{\partial y^2}\right)+\rho g_x \tag{1}$$

$$\rho\left(\frac{\partial V_y}{\partial t}+V_x\frac{\partial V_y}{\partial x}+V_y\frac{\partial V_y}{\partial y}\right)=-\frac{\partial p}{\partial x}+\mu\left(\frac{\partial^2 V_y}{\partial x^2}+\frac{\partial^2 V_y}{\partial y^2}\right)+\rho g_y \tag{2}$$

$$\rho c_p\left(\frac{\partial T}{\partial t}+V_x\frac{\partial T}{\partial x}+V_y\frac{\partial T}{\partial y}\right)=2\mu\left[\left(\frac{\partial V_x}{\partial x}\right)^2+\left(\frac{\partial V_y}{\partial y}\right)^2\right]+\mu\left[\left(\frac{\partial V_x}{\partial y}+\frac{\partial V_y}{\partial x}\right)^2\right] \tag{3}$$

$$\frac{\partial c}{\partial t}+V_x\frac{\partial c}{\partial x}+V_y\frac{\partial c}{\partial y}-\frac{\partial}{\partial x}\left(D_x\frac{\partial c}{\partial x}\right)-\frac{\partial}{\partial y}\left(D_y\frac{\partial c}{\partial y}\right)=0 \tag{4}$$

Equations (1) and (2) are the mass conservation equations in both the X-and Y, and Equation (3) is the thermal energy survival equation. Equation (4) is the dissipation and distribution relation obtained using the continuity equation, where ρ is the air Fluid Density, c is the water vapor concentration, and D is the disturbance mass transfer coefficient. Dx and Dy should be determined, and their molecular and efficient distributions should be considered. νx and νy indicate the speeds in the x and y directions, respectively. Evaluating the prevailing conditions of this study included higher Reynolds number in atmospheric flows, considering the effect of molecular viscosity insignificant, take into account the impact of the turbulent flow and eddy currents on distribution, proper pattern for modeling due to fit with above mention condition, strength, cost beneficial calculations and acceptable accuracy in wide range of turbulent flows, RNG K-ε were selected (Pope Stephen,B, 2007, 101-104). RNG K-ε turbulence model is another subset of K-Epsilon turbulence models. Among the K-Epsilon models, the RNG model provides better results than the standard mode in cases where the flow is under strong rotation, voracity and curvature. The K-Epsilon turbulence model compared to other models of the K-Epsilon family, when the flow It has reverse gradient or separation, it works very well. Also, compared to RNG turbulence model, using K-Epsilon model can bring better stability.

The equations established in this study are as follows:

$$\frac{Dk}{Dt}=\nabla.(\frac{\nu_T}{\sigma_k}\nabla k)+P-\varepsilon \tag{5}$$

$$\frac{\overline{D}\varepsilon}{\overline{D}t}=\nabla(\frac{\nu_T}{\sigma_\varepsilon}\nabla\varepsilon)+C_{1\varepsilon}\frac{\varepsilon}{k}P-C_{2\varepsilon}\frac{\varepsilon^2}{k} \tag{6}$$

$$\nu_t=c_\mu\frac{k^2}{\varepsilon} \tag{7}$$

where the constant coefficient Cμ is 0.0845 in the above equation. According to empirical observations and considering the stress relationship in the atmosphere, the value was determined to be 1.7.

The constant values in the model are as follows:

$$C_{1\varepsilon}=1/42 \ , \ C_{2\varepsilon}=1/68 \ \ \sigma_k=\sigma_\varepsilon=./72$$

In a volume-limited procedure for solving numerical equations, the survival rules apply to all variables at the control level. Thus, when the value determined from a standalone variable is transferred out of the control volume, the same amount enters the adjacent control volume. Thus, the production or artificial destruction of static variables could exist. This method is based on an integrated form of survival equations, and the Diegans–Goss case can be written as follows:

$$\frac{\partial}{\partial t}\left(\int_\forall \rho\phi d\forall\right)+\int_A n.(\rho\phi u)dA=\int_A n.(\Gamma\nabla\phi)dA+\int_\forall S_\phi d\forall \tag{8}$$

Where ⦰ corresponded to the relative velocity component and Γ and S⦰ means viscous and sentence source.

Using boundary condition and solve equations:

A 3200m long (north to sought direction) based on the standard and 5000m height (five times more than the mountain height) was taken as the resolution range. The origin coordinates on the ground surface were fitted 500 m before the mountain. The total calculation space was divided as a Tetrahedron, and the controlled number of volume and calculation time were optimized. The knowledge of higher changes in variables such as pressure, speed, etc. near the mountain range and finest control volume were used in that region to improve the calculation accuracy. Depicted geometric diagrams and dividing computing environments into smaller controlled volumes were created using the Gambit networking software.

Input temperature profile on the domain was determined by Monin Obukhov's similarity theory and gave to the main program by a sidelong program (Zannetti, 1990 and Jacobsen, 2005, 239-250): Temperature profile:

$$\overline{\theta_r}(y) = 281/7 \; - 0/00627\left[\ln \frac{y}{0/0007} - 2\ln \frac{1+\left[0/9 \; (1+0/0018y)^{-0/5}\right]^{-1}}{2/0} \right]$$

In this relation, y is the height parameter.

In the boundary entrance, because of the thermal profile and incomprehensible atmospheric input, flow conditions containing velocity were used, and in the external boundary, the boundary condition of fluid flow was used to equalize the fluid pressure to atmospheric pressure. For the upper geometry limitation, the symmetry of the boundary condition (all flows considered equal to 0 because of the insignificant amount and being away) and earth and mountain slope, the boundary condition of the wall is defined. The cloud entrance surface, which is considered as the flow input, contains the speed owing to the temperature and speed (Yang Lee, Etal 2007).

RESULTS & DISCUSSION

Preliminary, as shown in Figure 1, clouds remained unmoved at heights of 100 to 300m from the base of the valley, which typically occurred on special days of the season at the end of spring. The mass ratio of water vapor to air, environmental temperature, dew point temperature, and pressure were determined to be 0.63. Translocation could occur due to 5 °C thermal differences between the valley base and mountain slope up to a height of 500 m. This temperature difference causes vertical convective flow creation near the surface air. The results obtained by modeling showed that this heat was sufficient for cloud movement to the upper side and moved upward owing to convective air movement along the slope of the mountain. Calculations performed on the time interval of program outputs showed that a generation temperature difference

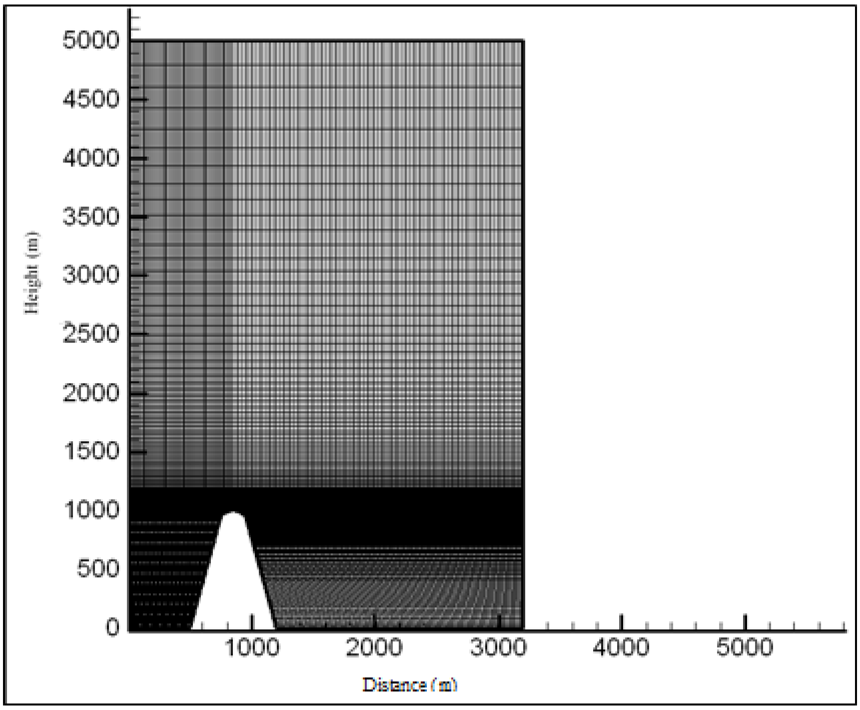

Fig. 1. presentation of a computational space with proper geometry

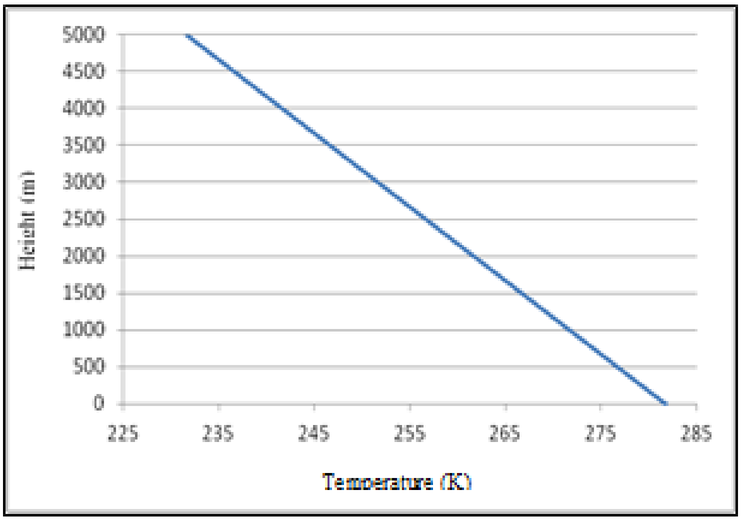

Fig. 2. The temperature profile of the region Modified for template input information

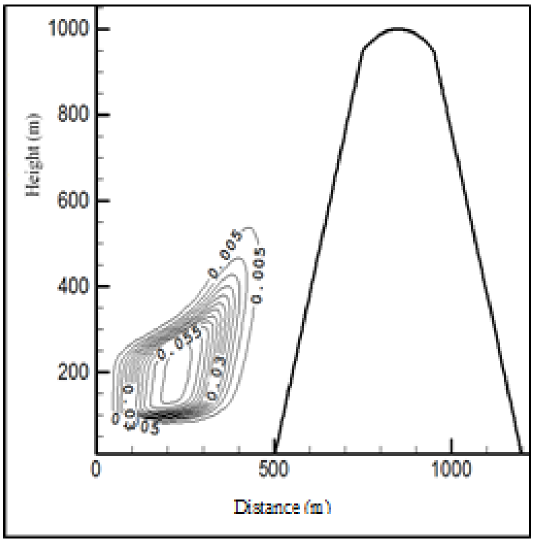

Fig. 3. clouds in the first moment of heat applying (The alignment lines represent the mass ratio)

of 10 °C (more than 5oC) could induce this movement, but was higher than 5 °C. Comparing these cases, it was concluded that at 5 °,Ca higher concentration of water vapor reached the upper level. For example, applying 10 °C water vapor required 9 min to reach the mountaintop, while the concentration declined to 69 percent. But with a 5-degree temperature difference, clouds reached after 13 min with a 43% reduction in concentration (Figure 3). Hence, given the importance of water vapor concentration in reducing cloud formation and rain, 5 °C was found to be more suitable for this transformation. In this case, as the temperature rose below the cloud and lowered the density, it climbed upward. After climbing, temperatures dropped and followed until the temperature of the cloud and the environment became equal or the ambient temperature exceeded the water vapor temperature; therefore, air ascent to the upper side stopped. Clouds dissipated because of speed creation and the presence of heat, so a lower mass percentage of water vapor is observable in the upper mountainous areas and decreases its homogeneity. As

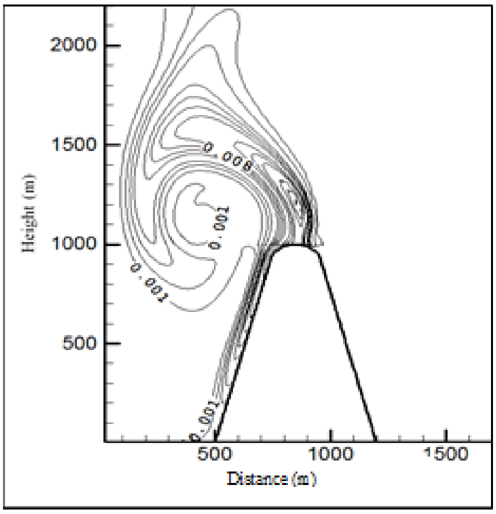

Fig. 4. clouds after 12 minutes and 54 seconds of heat application (The alignment lines represent the mass ratio)

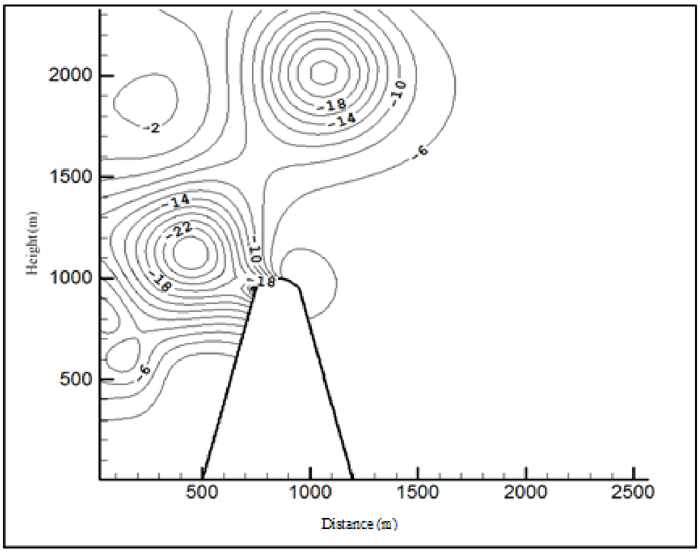

Fig. 5. pressure alignment line (Pa) after 12 minutes and 54 seconds of heat application

observed in Figure 3, after reaching clouds to higher levels, due to lower wind speed, which is unable to move clouds, they move down to the lower side. Coming down the clouds proved that because of a considerable reduction in pressure in the center of the convection focus because fluid movement took place from high-pressure places to lower pressure parts, clouds moved to these areas.

Considering the pressure and speed alignment lines, it can be observed in Figure 4 and 5 that convective motion begins with the starting heat and temperature differences resulting from the pressure difference. It moved from the high-pressure to low-pressure areas. The ground surface and mountain slope act as the heat and energy sources, respectively. Therefore, the pressure increased near these levels but at a lower speed, but was enhanced gradually by the start of the movement.

Getting away from the earth and mountain surfaces, as shown in Figure (7), the temperature reduced gradually and reached the ambient temperature. The temperature increased by 10 m but

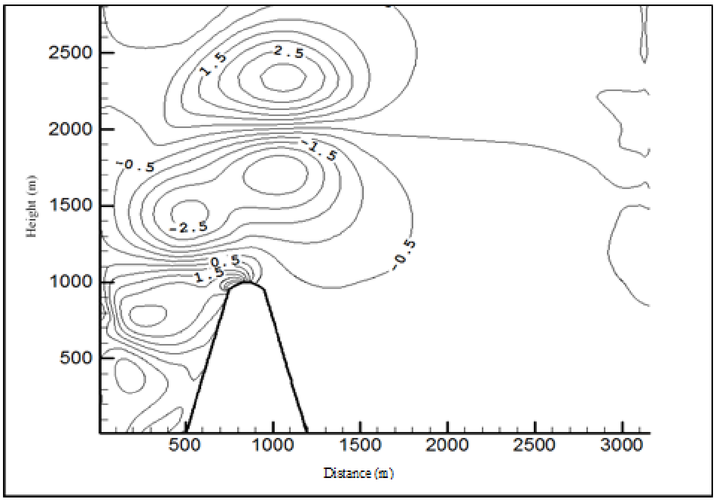

Fig. 6. speed alignment line (m/s) after 12 minutes and 54 seconds of heat application

Fig. 7. temperature alignment line (K) after 12 minutes and 54 seconds of heat application.

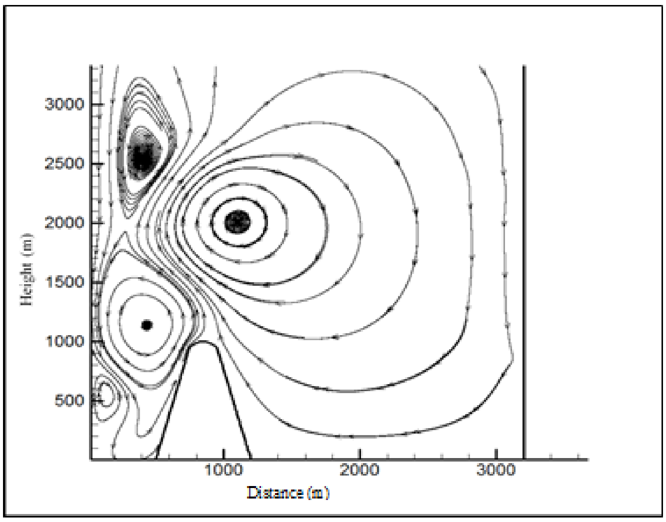

Fig. 8. flow lines after 12 minutes and 54 seconds of heat application.

then reached the ambient temperature.

Figure 6 shows the airflow lines after heat induction. Convection is generated in 3 zone due to the temperature difference; thus, the pressure difference is observable.

CONCLUSION

One of the main reasons which caused the climate change in the world is artificial thermal pollution of human activities. The main aim of proposed numerical model demonstrated that cloud movement and increase depend on temperature owing to thermal due to thermal pollution energy dissipated to the valley, environmental pressure, wind speed, cloud height position, and atmospheric stability degree. Because numerical modeling of the displaced cloud concentration is important, the reduction percentage of the density was calculated through translocation. The lower the difference in temperature, the more rapidly process declined, but a higher concentration of clouds reached the upper levels. Therefore, the optimum temperature difference for this displacement is the value that satisfies both the time and concentration aspects. Clouds climbed upward with air convection movement owing to temperature differences between the mountain slope and valley base through the steep. Meanwhile, the cloud becomes hotter owing to heat, lowers its density rather than air density increases. The upward movement continued until the heated air became coherent with the air at higher levels, after which the air dropped downward. If a slight wind that could move the clouds blow when clouds with air reach near the summit, clouds might be governed to another side. However, because of temperature differences caused by thermal pollution between clouds and air (clouds are warmer than air), clouds cooled again and flowed down the mountain over the slope. Considering all these issues, this model provides a good understanding of atmospheric motion and indicates that Fluent is a powerful software for modeling these movements. This model can be used for environmental goals such as cloud transmission for rainfall, tempering atmospheric conditions, and reforestation in arid and semi-arid areas.

GRANT SUPPORT DETAILS

The present research did not receive any financial support.

CONFLICT OF INTEREST

The authors declare that there is not any conflict of interests regarding the publication of this manuscript. In addition, the ethical issues, including plagiarism, informed consent, misconduct, data fabrication and/ or falsification, double publication and/or submission, and redundancy has been completely observed by the authors.

LIFE SCIENCE REPORTING

No life science threat was practiced in this research.

REFERENCES

Adler, C. (2020). High mountain summit: Outcomes and outlook. World Meteorological Organization Bulletin. Res., 69; 34–37.

Al-Ghrybawi, S., & Al-Jiboori, M. (2019). Study of surface heat inversions characteristics around Baghdad station. *Scientific Review Engineering and Environmental Sciences (SREES)*. Res., *28*(4); 610–618.

Al-Jiboori, M.H., & Jaber, S.H. (2018). The Study of Refractive-Index Structure Coefficient Behavior Derived from Two Weather Stations at Baghdad City. Al-Mustansiriyah Journal of Science. Res,. 29(4); 1-6.

Appel, K., Gilliam, R., Davis, N., Zubrow, A., & Howard, S. (2011). Overview of the atmospheric model evaluation tool (AMET) v1.1 for evaluating meteorological and air quality models. Environ Model Softw. Res., 26;434–443.

Boos, W. R., & Pascale, S. (2021). Mechanical forcing of the North American monsoon by orography. Nature. Res., 599(7886); 611–615.

Brümmer, B., & Schultze, M. (2015). Analysis of a 7-year low-level temperature inversion data set measured at the 280 m high Hamburg weather mast. Meteorol Z. Res., 24;481–494.

Bui, H. X. (2016). Impacts of vertical structure of large-scale vertical motion in tropical climate: Moist static energy framework. Journal of the Atmospheric Sciences. Res., 73(11); 4427–4437.

Chen, T., Guo, J., Tong, B., Cohen, J., Chen, X., Yun, Y., Lv, M., Guo, X., & Lee, S. (2022). Elucidating the impact of high- and low-pressure systems on temperature inversion from 9 years of radiosonde observations in Beijing. Atmos. Res., 271;106115.

Chernokulsky, A. (2019). Observed changes in convective and stratiform precipitation in Northern Eurasia over the last five decades. Environmental Research Letters. Res., 14(4); 45001.

Colle, B. A. (2013). Theory, observations, and predictions of orographic precipitation. In Mountain weather research and forecasting: Recent progress and current challenges. Springer. Res., 291–344.

Conway, D. (2019). The need for bottom-up assessments of climate risks and adaptation in climate-sensitive regions. Nature Climate Change. Res., 9(7); 503–511.

Czarnecka, M., Nidzgorska-Lencewicz, J., & Rawicki, K. (2019). Temporal structure of thermal inversions in Łeba (Poland). Theor Appl Climatol. Res., 136;1–13.

Davidson, C., & Spink, D. (2018). Alternate approaches for assessing impacts of oil sands development on air quality: a case study using the First Nation Community of Fort McKay. Journal of the Air and Waste Management Association. Res., 68(4); 308-328.

Dolatshahi, Z., Akbary, M., Alijani, B., & Toulabi Nejad, M. (2022). Analysis of temperature inversion in Ahwaz city.Arab J Geosci. Res., 15:1737. 1-15.

Dolatshahi, Z., Akbary, M., Alijani, B., & Toulabi Nejad, M. (2023). Statistical analysis of temperature inversion and its types in Birjand city using by inversion intensity index. J Geogr Res Desert Areas. Res., 11(1);18–35.

Elsen, P. R. (2020). Topography and human pressure in mountain ranges alter expected species responses to climate change. Nature Communications. Res., 11(1), 1974. 1-10.

EPA. (2023). United States environmental protection agency: Air pollutants criteria. Accessed 23 January 2023

Feng, X., Wei, S., & Wang, S. (2020). Temperature inversions in the atmospheric boundary layer and lower troposphere over the Sichuan Basin, China: climatology and impacts on air pollution. Sci Total Environ. Res., 726; 138579. 8963–8982.

Ghassami, T., Bidokhti, A., Sedaghat Kerdar, A., & Sahraian, F. (2010). Study of vertical potential temperature gradient during a few acute air pollution episodes in Tehran. J Environ Sci Technol. Res., 12(3);13–24.

Guédjé, F.K., Houéto, V.V.A., & Houngninnou, E. (2017). Features of the low–level temperature inversions at Abidjan upper-air station (Ivory Coast). Journal of Materials of Environmental Sciences. Res., 8(1); 264-272.

Hanberry, B. (2022). Global population densities, climate change, and the maximum monthly temperature threshold as a potential tipping point for high urban densities. Ecol Ind. Res., 135; 108512. 1-8.

Kermani, M., Jonidi Jafari, A., Gholami, M., Arfaeinia, H., Shahsavani, A., & Fanaei, F. (2021). Characterization, possible sources and health risk assessment of PM2.5-bound Heavy Metals in the most industrial city of Iran. J Environ Health Sci Eng. Res., 19;151–163.

Li, J., Chen, H., Li, Z., Wang, P., Cribb, M., & Fan, X. (2015). Low-level temperature inversions and their effect on aerosol condensation nuclei concentrations under different largescale synoptic circulations. Advances in Atmospheric Sciences. Res., 32(7); 898-908.

Miralles, D., Teuling, A., & van Heerwaarden, C. (2014). Mega-heatwave temperatures due to combined soil desiccation and atmospheric heat accumulation. Nature Geosci. Res., 7;345–349.

Odintsov, S., Miller, E., Kamardin, A., Nevzorova, I., Troitsky, A., & Schröder, M. (2021). Investigation of the mixing height in the planetary boundary layer by using sodar and microwave radiometer data. Environments. Res., 8(11);115. 1-15.

Pope Stephen, B. (2007). Turbulent Flows, Cornell University, Cambridge University Press.

Jacobson, M. (2005). Fundamentals of atmospheric modeling., Second edition., Cambridge University press.

Ramírez-Sánchez, H., García-Guadalupe, M., Ulloa-Gódinez, H., García-Concepción, O., Gutierrez, J., & Brito, S. (2013). Temperature inversions, meteorological variables and air pollutants and their influence on acute respiratory disease in the Guadalajara metropolitan zone, Jalisco, Mexico. J Environ Prot. Res., 4(08);142-153.

Rasilla, D., Martilli, A., Allende, F., & Fernández, F. (2023). Long-term evolution of cold air pools over the Madrid basin. Int J Climatol. Res., 43(1);38–56.

Sogno, P., Kuenzer, C., Bachofer, F., & Traidl-Hoffmann, C. (2022). Earth observation for exposome mapping of Germany: analyzing environmental factors relevant to non communicable diseases. Int J Appl Earth Obs Geoinf. Res., 114; 103084. 1-12.

Tavousi, T., & Hussein Abadi, N. (2016). Investigation of inversion characteristics in atmospheric boundary layer: a case study of Tehran, Iran. Model Earth Syst Environ. Res., 2;1–6.

Wang, W., Guo, X., Li, H., & Dong, X. (2018). Aerosols characteristics beneath the clouds based on airborne observation in early summer over sichuan basin. J. Arid Meteor. Res., 36 (2) 167-175.

Yang, L. (2007). Characterization and application of single fluorescent Nano diamonds as cellular biomarkers

Zannetti, P. (1990). Air pollution Modeling, Theories, Computational methods and available software, Computational mechanics Publication.